

Origins and evolution of stress development in sol-gel derived thin layers and multideposited coatings of lead titanate

S. S. Sengupta, S. M. Park,^{a)} D. A. Payne, and L. H. Allen

Department of Materials Science and Engineering, Seitz Materials Research Laboratory, and Beckman Institute, University of Illinois at Urbana-Champaign, Urbana, Illinois 61801

(Received 25 August 1997; accepted for publication 7 November 1997)

Stress development in thin layers of lead titanate prepared by sol-gel processing was monitored by *in situ* laser reflectance measurements. Layers were spin coated onto silicon substrates and thermally cycled to 500 °C. The shrinkage normal to the rigid substrate was determined by *in situ* ellipsometry. Changes that occurred on drying and firing, which related to densification and stress development, are reported. The observed changes were explained in terms of evaporation and solvent/polymeric network interactions at lower temperatures, and thermal expansion mismatch between the substrate and the coating after formation of the dense oxide. Crystallization into the perovskite structure occurred only in thicker or multideposited coatings, altering the state of stress from tensile, to progressively more compressive, on cooling. The importance of the choice of substrate material, deposition method and heat treatment conditions, in relation to stress development and dependent electrical properties, are discussed. © 1998 American Institute of Physics. [S0021-8979(98)04804-X]

I. INTRODUCTION

Thin layers deposited on substrates by solution methods can develop stresses on drying and firing. The substrate provides a mechanical constraint, which prevents free strain to develop in the plane of the coating. Thus, strain due to thermal expansion mismatch between the substrate and the coating, or due to phase transformations, is manifested as stress in the integrated layer on cooling to room temperature.

The presence of stress in ferroelectric thin layers can cause stress-related problems induced from the piezoelectric effect. In thin-layer form, ferroelectric $\text{Pb}(\text{Zr,Ti})\text{O}_3$ (PZT) offers key advantages for a wide variety of applications, such as integrated piezoelectric devices, nonvolatile memories and electro-optic modulators.¹⁻⁴ However, film stress can have a significant effect on mechanical, electrical, and optical properties, affecting the reproducibility of properties and the reliability of devices. In a study on rf-sputtered BaTiO_3 films, Desu⁵ claimed that increasing compressive stress resulted in higher coercive fields, lower remanent polarizations, and a shift in the Curie point to a higher temperature. While examining residual stress effects in sol-gel processed PZT coatings, Garino and Harrington⁶ observed an increase in the remanent polarization (by 11%) and dielectric constant (2%) when the tensile stress was lowered by ~30%. More recently, Spierings *et al.*⁷ reported on the stress development in a sol-gel derived PZT capacitor using Pt for the top and bottom electrodes. They found that on annealing the top electrode, the stress state in the underlying PZT layer (which had previously undergone a crystallization process) changed from tensile to compressive, with an attendant improvement in the switching properties. The tensile stress was believed to

stabilize domains oriented parallel to the plane of the layer; whereas compressive stresses generated in the PZT layer (on cooling through the Curie point) favored polarization alignment perpendicular to the layer. Removal of the top electrode, followed by reannealing of the PZT layer, restored polarization parallel to the layer, a result attributed to the prevailing "minimum energy" state in the absence of the top electrode. Earlier, Tuttle *et al.*⁸ used different substrate materials to illustrate similar behavior: sol-gel PZT coatings processed on MgO substrates developed compressive stresses on cooling through the Curie point, thus orienting domains with their "c" direction normal to the layer. Coatings deposited on platinized silicon substrates were always found to be in tension and thus exhibited type "a" behavior. Differences between thin layer and bulk properties were noted by Sengupta *et al.*⁹ for tin-modified PZT. The diffuse nature of dielectric transitions, and lower values of field-induced strains, obtained for solution-derived thin layers, were rationalized in terms of an internal-stress state existing in fine-grain microstructures.

Tensile stresses in thin layers can often lead to cracking or decohesion of the layer, rendering the coating unusable for insulating purposes. The magnitude of stress thus places a limit on the film thickness. Compressive stresses can in turn result in buckling of the film.

Sol-gel processing is widely used in the preparation and study of ferroelectric thin layers. Typically, the method involves deposition of a metalorganic precursor solution on a substrate by a spin- or dip-coating technique, followed by drying and firing of the layer to crystallize the functional phase. In addition to water and solvent loss, decomposition and pyrolysis of nonvolatile organic species during heat treatment results in constrained shrinkage and consequently a large tensile stress may build up in the coating during firing. Concurrent thermal expansion mismatch effects and phase

^{a)}Permanent address: Department of Materials Engineering, Hankuk Aviation University, Kyongki-Do, Korea.

transformations can further alter the magnitude or the state of stress. For example, for a silica layer deposited on a silicon substrate, Parill¹⁰ found that drying accounted for an increase in tensile stress to ~ 200 MPa at 200 °C. Further, removal of organics and bound OH groups resulted in the formation of additional $\equiv\text{Si}-\text{O}-\text{Si}\equiv$ linkages, raising the stress to 550 MPa at 500 °C. Fardad *et al.*¹¹ reported that a greater degree of hydrolysis of a silica sol before deposition lowered the eventual shrinkage and stress level after heat treatment between 400–500 °C, presumably due to a reduction in unreacted organic groups. Stress measurements carried out by Voncken *et al.*¹² on γ -AlOOH layers indicated a sharp increase in stress within several minutes of deposition, when held at 25 and 40 °C. The rapid buildup of stress was attributed to constrained shrinkage of the layer during drying. Residual stress analysis by Lakeman,¹³ on PZT coatings using x-ray diffraction methods, identified the development of a large tensile stress (~ 500 MPa) for constrained shrinkage during drying and firing. In a study reported by Boggs *et al.*,¹⁴ BaTiO₃ thin layers on Si/SiO₂ substrates were subjected to thermal cycling after deposition. During the heating cycle, plastic deformation of the coating was observed at lower temperatures, partially relieving the stress; on further heating, however, an almost linear response of stress was observed with increasing temperature, arising solely from thermal expansion mismatch between the substrate and the coating.

While the importance of stress control in solution-derived thin layers is obvious, few studies have focused on a fundamental understanding of stress development on heat treatment.^{10,12,15} The drying and firing processes can account for a large proportion of the total stress. In particular, drying imposes strong capillary forces on the gel network as liquid from within the pores evaporates, creating new liquid–vapor interfaces. In this article, we present a systematic study of the evolution of stress in sol-gel derived thin layers of lead titanate, with emphasis on drying and consolidation mechanisms. Shrinkage data are introduced to further clarify the densification mechanisms in the thin layers.

Several techniques have been reported for the determination of stresses in coatings. These include spectroscopic methods (which detect shifts in vibrational frequencies arising from stressed lattices) such as Raman^{16,17} or optical fluorescence,¹⁸ x-ray diffraction,^{13,17} cantilever beam deflection^{12,15} and wafer curvature measurements.^{8,19} In the present study, stresses were measured using a laser reflectance method described below.

II. EXPERIMENTAL PROCEDURE

Precursor solutions of lead titanate (PT) were prepared according to the method developed by Budd *et al.*²⁰ Molar solutions were partially hydrolyzed under neutral conditions in an equal volume of a water/alcohol mixture using $R_w = 1$ (where R_w is defined as the molar ratio of water to mixed metal alkoxide), and aged for a period of one to a few days at room temperature (RT). The time of aging did not appear to have any significant effect on subsequent shrinkage behavior

and stress development. Thin layers were spin cast onto bare Si substrates with a surface native oxide layer about 50 Å thick.

Specimens for stress experiments were prepared by spin coating the sol onto 3 in. diam Si (100) substrates. Uniformity was achieved by allowing the sol to coat the entire wafer at low rpm before slowly increasing the spin speed to 3000 rpm for 50 s. To improve increased sensitivity to bending stress, thin (75 μm) wafers were selected. As-deposited layers were then subjected to various thermal cycles in air with simultaneous stress measurements. In order to account for the variation of layer thickness with temperature cycling, *in situ* ellipsometric measurements were carried out separately on single layers coated on smaller substrates, using a fixed wavelength Gaertner L116C ellipsometer. Each specimen was subjected to an identical thermal cycle as the corresponding stress wafer, with continuous thickness monitoring. Experimental details of the measurement procedure are given elsewhere.²¹ Both stress and ellipsometric measurements were initiated within 10 min of deposition of a layer.

In sol-gel processing, repeated deposition and consolidation of single layers is generally employed to build up a thicker coating necessary for many applications. A combined investigation of stress development in multideposited layers was therefore undertaken for lead titanate deposited on silicon by the sol-gel method. Each as-spun layer was subjected to a RT–500 °C–RT thermal cycle at 3 °C/min with *in situ* stress determination, before subsequent depositions. A total of ten depositions were made. In addition, layers were separately deposited on smaller substrates and heat treated under identical conditions to examine the evolution of structure for multiple depositions. An x-ray diffractometer (Rigaku D/Max IIIA, Cu K_α radiation) was used for this study.

III. STRESS MEASUREMENT

Stress was determined using a Tencor FLX-2300 equipped with a laser reflectance measurement system. The radius of curvature of the wafer was found by measuring the angle of reflection of the laser beam normal to the surface. The stress was then calculated according to the Stoney equation²²

$$\sigma = \left(\frac{E}{1-\nu} \right)_s \frac{t_s^2}{6t_c} \left(\frac{1}{R} - \frac{1}{R_0} \right), \quad (1)$$

where $(E/1-\nu)_s$ is the biaxial elastic modulus of the substrate, t_s and t_c are the substrate and coating thicknesses, respectively, R is the radius of wafer curvature measured during thermal cycling, and R_0 is the reference radius of curvature (prior to deposition). The above derivation, based on beam bending mechanics, assumes a layer thickness much less than the substrate thickness. Under these conditions, the elastic properties of the coating are not required for the determination of stress.

For the multiple depositions, since each layer was spin cast on an already densified coating, the “multilayer,” or multideposited layer, could be represented as a composite structure consisting of a drying layer densifying over a coating of constant thickness; in which the stress was governed

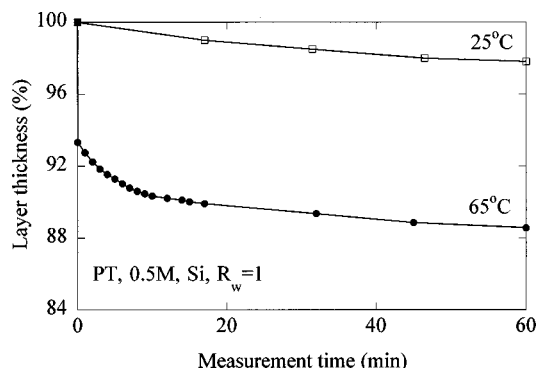


FIG. 1. Thickness as a function of time for a single layer at 25 and 65 °C.

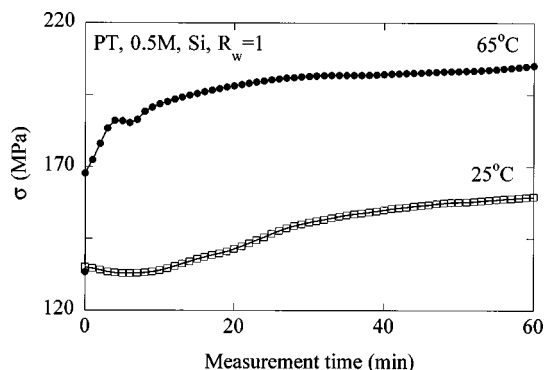


FIG. 3. Stress development with time for a single layer at 25 and 65 °C.

principally by the thermal expansion mismatch between the layer and the coating (and any possible phase transformations). For an n -layered coating, each deposition imposes a separate bending moment and separate contribution to the curvature. Since a summation of the moments can be reduced to a sum of individual curvatures, the expression relating the total stress in the coating to the stress developed in each deposited layer can be written as

$$\sigma_c t_c = \sum_{i=1}^n \sigma_i t_i, \tag{2}$$

where σ_i and t_i refer to the stress generated within the thickness of the i th layer, and σ_c and t_c are the corresponding values for the composite coating. Thus, the total thickness t_c on heating was accounted for by $(n-1)$ dense layers of a constant thickness t_d (corresponding to the value obtained after heat treatment to 500 °C), and a densifying top layer of a temperature-dependent thickness t_{top} . In other words, on heating, the thickness of the coating was a function of temperature (T), according to

$$t_c(T) = (n-1)t_d + t_{top}(T) \tag{3}$$

while on cooling, the thickness was assumed constant, given by

$$t_c = n t_d. \tag{4}$$

The stress σ_c was then calculated from Eq. (1).

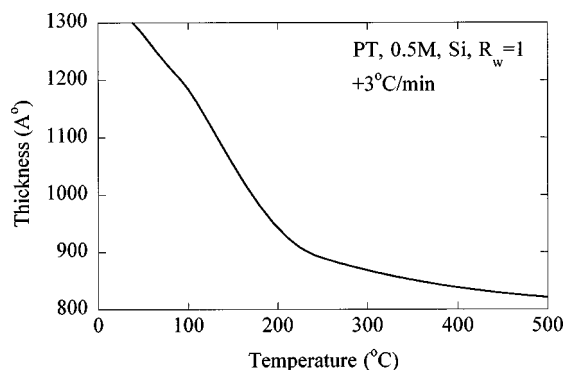


FIG. 2. Shrinkage as a function of temperature for a single layer up to 500 °C.

IV. RESULTS

A. Shrinkage behavior

A single as-deposited PT layer, characterized by ellipsometry, was typically 1300 Å thick with a refractive index $n=1.9$. At low temperatures (below ~ 100 °C), t_c and n were found to vary with time when held at a particular temperature. Figure 1 shows the variation of thickness, as a function of time, at room temperature (RT) and at 65 °C. The shrinkage for a layer heated at a constant rate of 3 °C/min from room temperature up to 500 °C is illustrated in Fig. 2. These results indicate that a considerable amount of shrinkage takes place during solvent removal, and continues up to ~ 200 °C.

B. Stress development on drying and firing

An as-spun layer always developed a tensile stress on deposition. The magnitude of the stress was dependent on the deposition conditions, i.e., spin speed, viscosity of sol, humidity, etc. Figure 3 gives the corresponding variation of stress with time for the as-deposited coatings reported in Fig. 1. These data indicate that substantial drying occurred at low temperatures with time, resulting in a steady increase in stress attributable to constrained shrinkage. Stress changes arising from the constant heating and cooling rates (see Fig. 2 for corresponding shrinkage data) are given in Fig. 4. Note that the stress was always tensile for a single layer deposition.

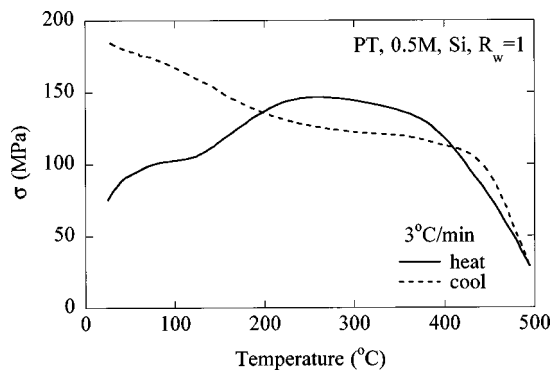


FIG. 4. Stress development on thermal cycling for a single layer on silicon.

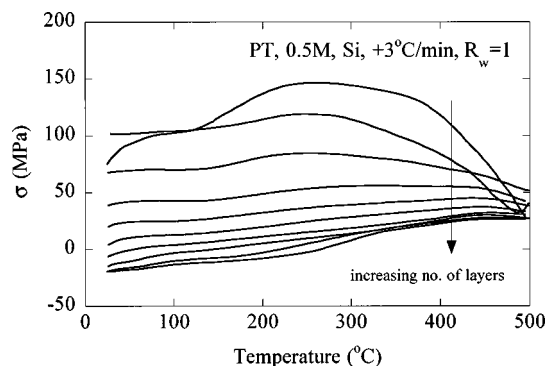


FIG. 5. Stress development on heating for multideposited layers.

C. Multiple depositions

Based on calculations obtained using Eqs. (1)–(4), the total stress in the coating was determined for both heating and cooling cycles. Figure 5 illustrates stress development on heating to 500 °C, after deposition of each new layer. The corresponding cooling data are given in Fig. 6.

V. DISCUSSION

A. Single layer

Deposition of a thin layer by spin coating involves rapid loss of solvent by evaporation during the process. The resulting layer is generally more dense than a gel prepared from the same sol. Evaporation of liquid from within the polymeric network creates tension in the liquid due to the concave menisci developed at the liquid–vapor interface.²³ The liquid tension forces the compliant network into compression. The total stress in the layer is then approximately equal to the capillary pressure or tension exerted by the liquid. Solvent loss continues, however, long after deposition even at low temperatures, as indicated in Fig. 1. Comparison of the shrinkage behavior observed at the two temperatures indicates a similar trend in the development of shrinkage after deposition. The initial shrinkage of ~7% observed at 65 °C corresponds to an instantaneous temperature ramp from 25 to 65 °C. During this short interval, solvent from inside the pore structure of the network would be rapidly expelled, resulting in constrained shrinkage for the coating. Compression of the network would reduce the pore size, further increasing the capillary pressure, and hence the stress, in the

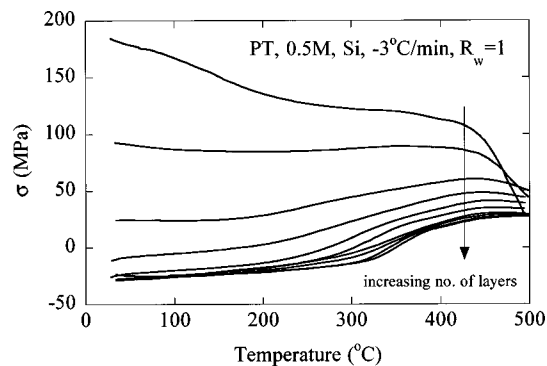


FIG. 6. Stress development on cooling for multideposited layers.

plane of the coating (see Fig. 3). Following the accelerated drying period for the coating at 65 °C (about 8–10 min after the temperature transient), both isothermal holds appeared to produce equivalent shrinkage and stress variations with time. This is not unexpected, since both networks are compliant under the influence of capillary forces at this stage. The slight relaxation of stress, observed initially in both coatings, might be due to adsorption of water, or solvent, at the pore liquid–vapor interface.

The constant heating rate experiments serve to illustrate the various mechanisms operative during the drying and firing processes. As seen in Fig. 4, the tensile stress generated in the as-deposited coating increased steadily until ~80 °C. During this time, liquid would be continuously drawn from within the pores to replenish that lost by evaporation at the pore surface. The accompanying capillary forces act to plastically deform the network.

Contraction of the network would also result in a closer approach of incompletely reacted metalorganic groups. Thus, condensation between groups would also be enhanced, serving to crosslink the network. This process would lead to a reduction in the effective pore size, thereby increasing the capillary forces even further. However, crosslinking increases the stiffness of the network. These two opposing factors would determine the extent of stress behavior above ~100 °C. Expulsion of solvent species, produced by polycondensation reactions and additional network contraction, would account for the shrinkage in this temperature regime. Eventually, the network would develop sufficient strength to withstand the compressive forces imposed by the liquid, causing the remaining liquid to recede into the minute pores. The capillary pressure is a maximum at this stage.²³ At higher temperatures, pyrolysis of organic material would contribute to increasing shrinkage. The constrained shrinkage of the stiff network would induce large stresses in the coating.

Beyond ~220 °C, relatively little shrinkage was observed. This is in contrast to the behavior of bulk gels²⁴ where pyrolysis is followed by significant shrinkage due to structural relaxation. Initially, a thin layer is more dense and less crosslinked than an equivalent gel, allowing greater rearrangement of the polymer groups due to solvent evaporation during spin casting. The low water content of sols used for layer deposition also limits crosslinking, resulting in low viscosity, and consequently a higher densification rate for the coating. Shrinkage of a layer was therefore almost complete by ~220 °C. A more extensive report on densification behavior in PT thin layers is underway.²⁵

In the case of lead-based perovskites, lead loss due to volatilization of PbO and interdiffusion between the coating and the substrate, at higher temperatures, can occur. This issue has been addressed in a previous paper²¹ and the above effects were not observed for a single PT layer. Hence, the stress behavior beyond 220 °C, and on cooling, was dominated by the thermal expansion mismatch between the oxide layer and the substrate, according to²⁶

$$\sigma_c = \int \left(\frac{E}{1-\nu} \right) (\alpha_s - \alpha_c) dT, \quad (5)$$

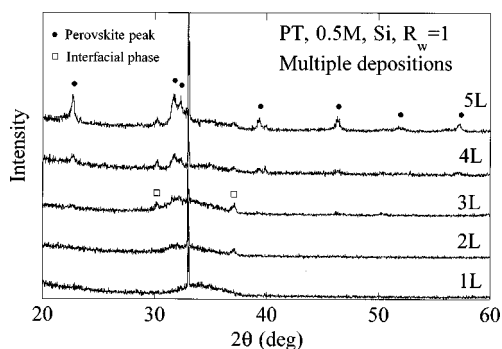


FIG. 7. X-ray diffraction data for multideposited layers on silicon after thermal cycling each layer between RT and 500 °C (1L=1 layer coating, 2L=2 layer coating, etc.).

where $(E/1-\nu)$ is the biaxial modulus of the layer coated, and α_s, α_c refer to the linear thermal expansion coefficient of the substrate and the layer, respectively. The gradient of the stress-temperature curve can then be used to determine the expansion coefficient of the coating. Our preliminary results on PZT 70/30 and lead zirconate (PZ) compositions follow anticipated trends: the expansion coefficient of the oxide is lower than that of silicon in either case ($\alpha_{PZ} < \alpha_{PZT} < \alpha_{Si} < \alpha_{PT}$), and the stress increases steadily on heating to 500 °C.

B. Multiple layers

When multiple depositions of layers of comparable thickness are formed on a substrate, such that the total coating thickness is much less than the substrate thickness, the total stress is affected by the stress developed in each layer, as explained previously. If the stress response for each subsequent layer were identical to that of the first, the composite stress could easily be predicted for the multideposited coating. In fact, the stress curve on cooling (when no further shrinkage occurs) for the n -layered structure would follow closely the cooling curve of the first deposited layer. In reality, the cooling curves for two or more layers, indicated in Fig. 6, were significantly different from the stress behavior of the first layer. The difference can be attributed to the difference in expansion coefficient between the multilayer and the single layer. For the latter, the PT layer would be on Si; for the former, the PT layer would be on a previously deposited PT layer. Closer examination of Fig. 6 indicates that with increasing number of depositions, the stress curves converge to constant behavior. The results indicate that the deposition of additional layers, followed by heat treatment to 500 °C, altered the single layer amorphous structure into a stable phase; effecting a substantial change in the expansion coefficient and consequently the stress state for the coating as a whole.

X-ray diffraction patterns for the first five layers are shown in Fig. 7. The first layer appeared amorphous, as suggested above. The measurement is sensitive enough to detect crystalline phases at this thickness; a separate experiment on a single PT layer deposited on *platinized* silicon revealed the presence of distinct perovskite peaks. Returning to Fig. 7, with increasing number of layers deposited and associated

heat treatments, the perovskite phase began to form, as evidenced by the appearance and sharpening of the perovskite peaks. After deposition of ten layers, the coating was almost completely crystalline. The emergence of two small peaks at $2\theta \sim 30.2^\circ$ and $2\theta \sim 37^\circ$ in multideposited specimens can be attributed to the formation of a small amount of a lead silicate phase,²⁷ and is considered below.

The stress behavior can now be rationalized in terms of structural changes that occur with increasing thickness for lead titanate depositions on silicon. The amorphous native oxide layer on the substrate's surface probably cannot provide favorable sites for nucleation of the perovskite phase during the initial heat treatment of the first layer. At the same time, the small thickness of the coating at this point limits homogeneous nucleation within the layer. On heating the second deposited layer, perovskite crystallites begin to form; this may be due partly to enhanced homogeneous nucleation in the thicker coating. Moreover, the amorphous PT layer may act to induce nucleation of crystallites at the interface between the two layers. Deposition and thermal cycling of additional layers further increases the relative amount of the crystalline phase. An inspection of the heating curves (Fig. 5) indicates a gradual suppression in variations as the thickness increases; suggesting that a smaller contribution to the stress results from drying of a layer, on a thicker densified coating. It must also be noted that extended high temperature heat treatment can stimulate interdiffusion reactions between lead oxide and silica at the substrate/coating interface.^{28,29} In our case, repeated thermal cycling at 500 °C resulted in the formation of a crystalline lead silicate phase referred to above. In any event, the volume fraction of this phase is small and the relative amount decreases for thicker coatings. A similar behavior has been reported for PZT layers deposited on quartz substrates.³⁰

This article has been concerned with stress evolution in single and multideposited lead titanate layers on bare silicon. When *platinized* silicon substrates are used, perovskite lead titanate forms more readily³¹ and can be expected to influence the stress response on further heating and cycling. Domain formation and electrical properties of ferroelectric thin layers are affected by the magnitude and sign of the stress. The state of stress, in turn, can be manipulated using appropriate substrate/electrode combinations. Stress development for multiple depositions of different materials undergoing various thermal treatments is an important topic and worthy of further study for integrated electromechanical thin layers.

VI. SUMMARY

Lead titanate coatings deposited by a chemical solution sol-gel method exhibited significant shrinkage on drying and firing. While most of the solvent evaporation occurred during spin coating, measurable shrinkage due to solvent loss was detected after extended time at room temperature. Constrained shrinkage of almost 40% occurred normal to the substrate during firing, and accounted for significant changes in the stress state. Thermal expansion mismatch between the coating and the substrate dominated the stress behavior on cooling.

The actual stress developed in a layer formed by multiple depositions was found to depend on the structure of the formed coating. As the thickness of the formed coating increased by successive depositions, crystallization of the perovskite phase from the amorphous oxide gradually changed the stress state from tension to compression on cooling to room temperature. The evolution of structure in thin layers was influenced by the choice of the substrate, the deposition technique, and the heat treatment conditions. These factors affected the stress development in coatings formed by multiple depositions. A single layer ($\sim 800 \text{ \AA}$) had a residual tensile stress of $\sim 200 \text{ MPa}$, whereas a multilayer (>5 layers) developed a residual compressive stress of $\sim 20 \text{ MPa}$. These changes could be important for variations observed in properties for stress-sensitive devices (e.g., integrated ferroelectric memories).

ACKNOWLEDGMENTS

The research was supported by the Basic Energy Sciences Division, U.S. Department of Energy, under Grant No. DEFG02-91ER45439. The use of facilities in the Center for Microanalysis of Materials at the University of Illinois is gratefully acknowledged.

- ¹R. E. Newnham and G. R. Ruschau, *J. Am. Ceram. Soc.* **74**, 463 (1991).
- ²C. A. Paz de Araujo and G. W. Taylor, *Ferroelectrics* **116**, 215 (1991).
- ³C. E. Land, *J. Am. Ceram. Soc.* **72**, 2059 (1989).
- ⁴S. K. Dey, D. A. Payne, and K. D. Budd, *IEEE Trans. Ultrason. Ferroelectr. Freq. Control* **35**, 80 (1988).
- ⁵S. B. Desu, *Phys. Status Solidi A* **141**, 119 (1994).
- ⁶T. J. Garino and M. Harrington, *Mater. Res. Soc. Symp. Proc.* **243**, 341 (1992).
- ⁷G. A. C. M. Spierings, G. J. M. Dormans, W. G. J. Moors, M. J. E. Ulenaers, and P. K. Larsen, *J. Appl. Phys.* **78**, 1926 (1995).
- ⁸B. A. Tuttle, J. A. Voigt, T. J. Garino, D. C. Goodnow, R. W. Schwartz,

- D. L. Lamppa, T. J. Headley, and M. O. Eatough, in *Proceedings of the IEEE 8th International Symposium on Applied Ferroelectrics* (IEEE, New York, 1992), pp. 344–348.
- ⁹S. S. Sengupta, D. Roberts, J.-F. Li, M. C. Kim, and D. A. Payne, *J. Appl. Phys.* **78**, 1171 (1995).
- ¹⁰T. M. Parill, *J. Mater. Res.* **9**, 723 (1994).
- ¹¹M. A. Fardad, E. M. Yeatman, E. J. C. Dawnay, M. Green, and F. Horowitz, *J. Non-Cryst. Solids* **183**, 260 (1995).
- ¹²J. H. L. Voncken, C. Lijzenga, K. P. Kumar, K. Keizer, A. J. Burggraaf, and B. C. Bonekamp, *J. Mater. Sci.* **27**, 472 (1992).
- ¹³C. D. E. Lakeman, Ph.D. thesis, University of Illinois at Urbana-Champaign, 1994.
- ¹⁴K. E. Boggs, D. L. Wilcox, D. A. Payne, and L. H. Allen, *MCM Proc.* (1994), p. 350.
- ¹⁵K. Keizer, K. P. Kumar, C. Lijzenga, V. T. Zaspalis, and A. J. Burggraaf, *Key Eng. Matls.* **61, 62**, 433 (1991).
- ¹⁶G. J. Exarhos and N. J. Hess, *Thin Solid Films* **220**, 254 (1992).
- ¹⁷E. Ching-Prado, A. Reynés-Figueroa, R. S. Katiyar, S. B. Majumder, and D. C. Agrawal, *J. Appl. Phys.* **78**, 1920 (1995).
- ¹⁸Q. Ma and D. R. Clarke, *J. Am. Ceram. Soc.* **76**, 1433 (1993).
- ¹⁹C. C. Li and S. B. Desu, *J. Vac. Sci. Technol. A* **14**, 1 (1996).
- ²⁰K. D. Budd, S. K. Dey, and D. A. Payne, *Br. Ceram. Proc.* **36**, 107 (1985).
- ²¹S. S. Sengupta, S. M. Park, and D. A. Payne, *Integrated Ferroelectrics* **14**, 193 (1997).
- ²²G. G. Stoney, *Proc. R. Soc. London A* **82**, 172 (1909).
- ²³C. J. Brinker and G. W. Scherer, in *Sol-Gel Science: The Physics and Chemistry of Sol-Gel Processing* (Academic, New York, 1990), Chap. 8.
- ²⁴C. J. Brinker, G. W. Scherer, and E. P. Roth, *J. Non-Cryst. Solids* **72**, 345 (1985).
- ²⁵S. M. Park, S. S. Sengupta, and D. A. Payne (unpublished).
- ²⁶M. Ohring, in *The Materials Science of Thin Films* (Academic, New York, 1992), Chap. 9.
- ²⁷The closest match can be found with a Pb_2SiO_4 phase: JCPDS Card No. 13-0279.
- ²⁸R. A. Roy and K. F. Etzold, *J. Mater. Res.* **7**, 1455 (1992).
- ²⁹Y. Shichi, S. Tanimoto, T. Goto, K. Kuroiwa, and Y. Tarui, *Jpn. J. Appl. Phys., Part 1* **33**, 5172 (1994).
- ³⁰S. B. Majumder, V. N. Kulkarni, Y. N. Mohapatra, and D. C. Agrawal, *Bull. Mater. Sci.* **17**, 1005 (1994).
- ³¹C. J. Lu, H. M. Shen, J. S. Liu, and Y. N. Wang, *J. Phys. D* **30**, 2338 (1997).